

# Using the Surface Features of Plant Matter to Create All-Polymer Pseudocapacitors with High Areal Capacitance

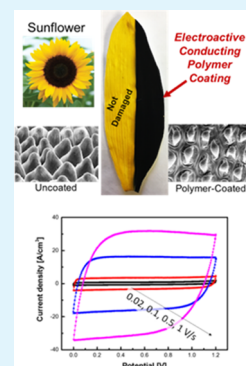
Lushuai Zhang and Trisha L. Andrew\*<sup>✉</sup>

Departments of Chemistry and Chemical Engineering, University of Massachusetts Amherst, Amherst, Massachusetts 01003, United States

## Supporting Information

**ABSTRACT:** Controlling mesoscale organization in thick films of electroactive polymers is crucial for studying and optimizing charge and ion transport in these disordered materials. Conventional approaches focus on directing long-range polymer aggregation and/or crystallization during film formation by using interfaces, flow and/or shear forces. Here, we describe an alternative method that takes advantage of naturally textured biological substrates and vapor-coating to structure thick-conjugated polymer films. Reactive vapor-coating is a technique that enables in situ synthesis of doped conjugated polymers inside a reduced-pressure reactor. Reactive vapor deposition conformally coats the surface of plant matter, such as leaves and flower petals, with conducting polymer films while leaving these living substrates undamaged. Importantly, the intricate surface features of plant matter are faultlessly reproduced in the coating, effectively creating thick, high-surface-area, electrochemically active conducting polymer electrodes on plant matter. A microstructured, 10  $\mu\text{m}$  thick film of p-doped poly(3,4-ethylenedioxythiophene) on a pilea involucrata leaf acts as an all-polymer pseudocapacitor with a higher areal capacitance (142  $\text{mF}/\text{cm}^2$ ) than an analogous film on a planar plastic substrate lacking microstructure (50  $\text{mF}/\text{cm}^2$ ). Taken together, reactive vapor deposition and microstructured plant matter present a unique combination of processing technique and substrate that can yield a diverse library of controllably microstructured electronic polymer films.

**KEYWORDS:** biorenewable substrate, conjugated polymer, reactive vapor deposition, pseudocapacitor, areal capacitance, flexible electronics



## INTRODUCTION

Electrochemical capacitors (ECs) are a promising subset of energy-storage devices that are well suited for integrating with a variety of portable energy-harvesting technologies.<sup>1–13</sup> ECs are subdivided into electrochemical double-layer capacitors, which depend on surface ion adsorption for charge storage and pseudocapacitors, which use fast redox reactions to store charge.<sup>1–4</sup> Redox-active (i.e., pseudocapacitive)-conjugated polymers possess advantageous mechanical properties that can, in theory, enable lightweight, flexible charge-storage technologies.<sup>14–19</sup> However, despite creative optimizations of structure, composition, and processing conditions,<sup>20–22</sup> all-polymer and/or polymer-composite electrodes have not matched the charge-storage capacity of double-layer capacitors made with various carbon allotropes and/or two-dimensional materials.<sup>23</sup>

A major limitation is that only thin polymer films (<100 nm), or “low mass loading”, can be used to create functional electrodes<sup>14–19</sup> because effective strategies to control and optimize mesoscale (micron-millimeter) structure in thick polymer films are unknown. In turn, low mass loadings limit the maximum attainable capacitance and energy/power density of polymer-based devices. To increase the electrochemical capacitance of all-polymer electrodes, selected investigations have focused on enlarging the electrode surface area by creating thin polymer films on electrically conductive, three-

dimensional scaffolds.<sup>20,24,25</sup> Though interesting, these strategies fail to fundamentally address the low mass loading limitation of polymer electrodes: as polymer coating thicknesses are increased past approximately 100 nm, bulk properties start to dominate and high internal resistances are inevitably manifested.<sup>23</sup>

In this report, we demonstrate that biological substrates can be used to impart mesoscale organization in thick (greater than 1  $\mu\text{m}$ ), electroactive polymer films. Reactive vapor deposition is a technique that enables in situ synthesis of doped conjugated polymers inside a reduced-pressure reactor and nondestructively creates conformal conducting polymer coatings on judiciously chosen, textured plant matter. Conducting polymer-coated flower petals and plant leaves act as all-polymer, pseudocapacitive electrodes that display higher areal capacitances as compared to analogous electrodes created on conventional, planar plastic substrates. Taken together, reactive vapor deposition and microstructured plant matter present a unique combination of processing technique and device substrate with the potential to create lightweight and portable charge-storage solutions.

Received: July 24, 2018

Accepted: October 18, 2018

Published: October 18, 2018

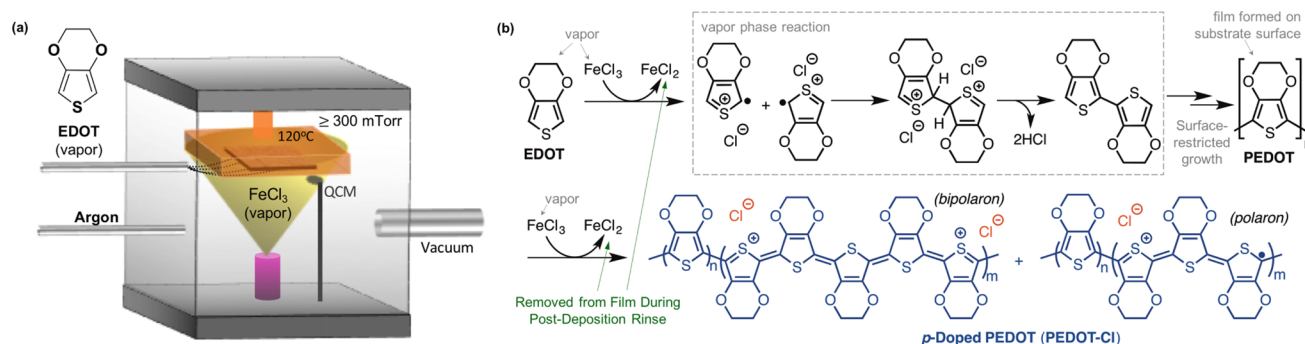


**Figure 1.** (a) Illustration of reactive vapor deposition chamber. (b) Reaction sequence during reactive vapor deposition and structure of persistently p-doped conducting polymer film used as a pseudocapacitor.

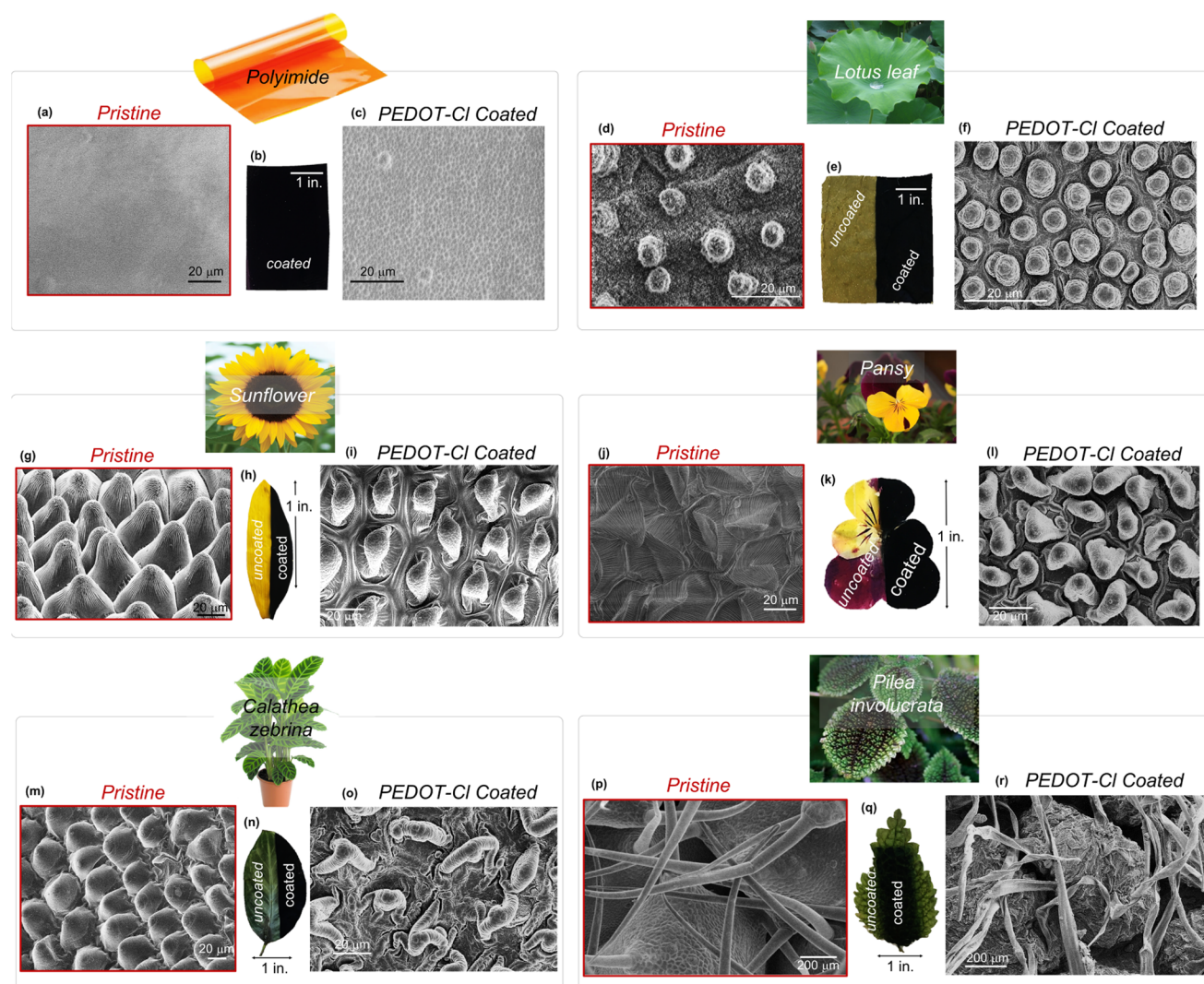


**Figure 2.** Vapor-deposited conducting polymer coatings on plant matter. (a–c) Smooth, flexible polyimide film substrate. (d–f) Lotus leaf substrate. (g–i) Sunflower petal substrate. (j–l) Pansy petal substrate. (m–o) Calathea zebrina leaf substrate. (p–r) Pilea involucreta leaf substrate. For each panel: (left) scanning electron microscope (SEM) image of a pristine substrate, (center) optical images of a partly coated sample, (right) SEM image of the substrate coated with a 10  $\mu\text{m}$  thick film of PEDOT-Cl.

## RESULTS AND DISCUSSION

Reactive vapor deposition of persistently p-doped poly(3,4-ethylenedioxythiophene) (PEDOT-Cl) is carried out in a previously reported, custom-built reactor (Figure 1).<sup>26,27</sup> The monomer, 3,4-ethylenedioxythiophene (EDOT) and oxidant, iron(III) chloride, are simultaneously introduced as vapors into

a stainless steel chamber held at 300–500 mTorr, where surface-restricted oxidative polymerization proceeds.<sup>26,27</sup> A higher flow rate of the oxidant, as compared to the monomer, is typically used to afford p-doped conducting polymer films. A postdeposition rinse effectively removes excess oxidant, residual oligomers, and other metal byproducts from the

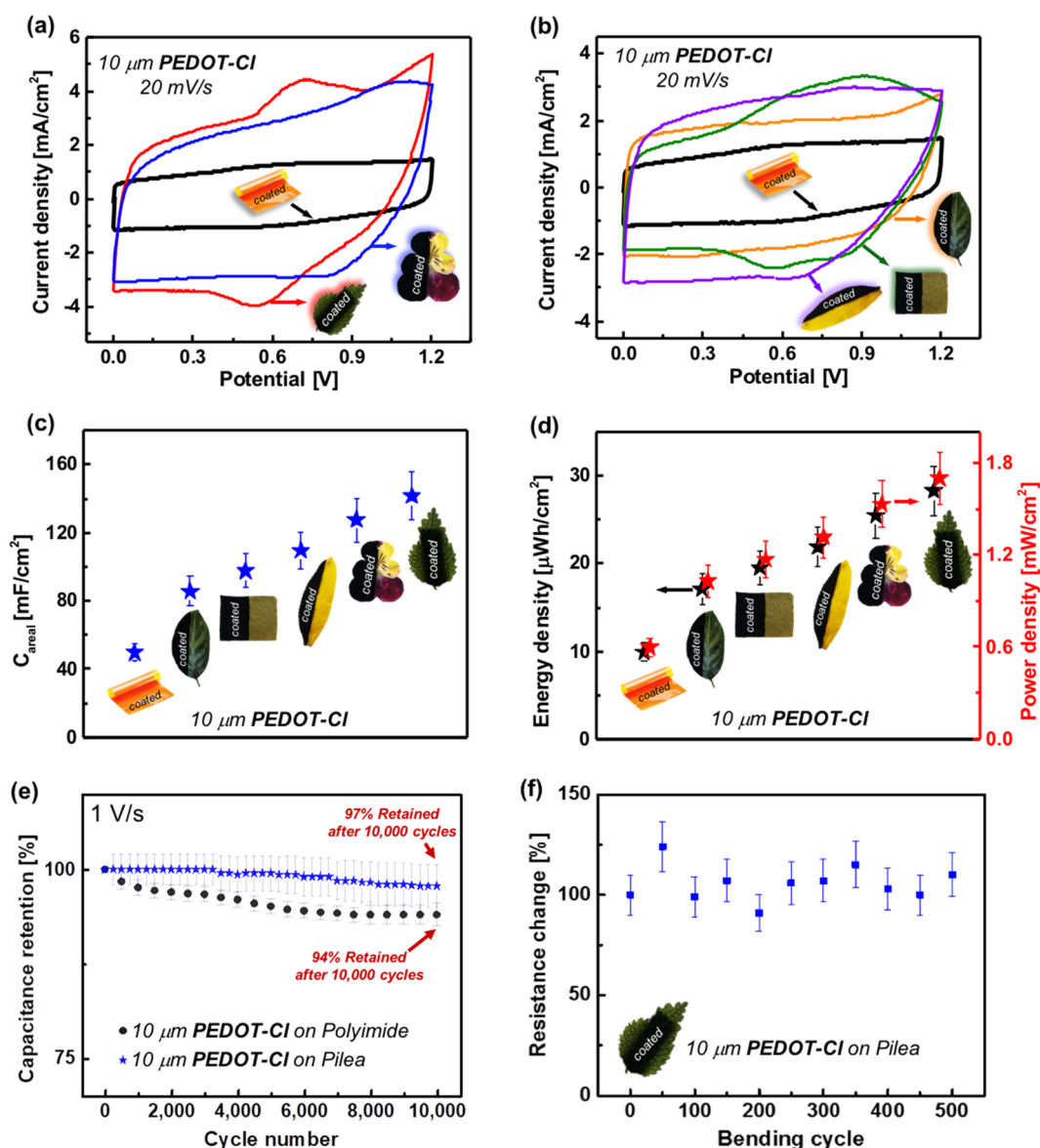


**Figure 3.** Symmetric-electrode pseudocapacitors. (a, b) Cyclic voltammograms of various symmetric-electrode, all-polymer pseudocapacitors in aqueous sulfuric acid electrolyte at a scan rate of 20 mV/s. The electrodes are polyimide, plant leaf, or flower petal substrates vapor-coated with a 10 μm thick film of PEDOT-CI. Current densities are normalized to the total electroactive area of each substrate. (c) Areal capacitance of symmetric-electrode pseudocapacitors. (d) Areal energy density and power density of symmetric-electrode pseudocapacitors calculated from cyclic voltammograms. (e) Charge–discharge cycle stability of symmetric-electrode pseudocapacitors measured at a scan rate of 1 V/s in aqueous sulfuric acid electrolyte. (f) Bending stability of a PEDOT-CI-coated pilea involucrata leaf electrode. The bending angle is 10°.

films (Figure S1), while minimally altering their doping level, as previously reported.<sup>27</sup>

A 10 μm thick, redox-active PEDOT-CI film<sup>27</sup> is used throughout this report to maximize the mass loading of the electroactive material and because that is the thickest coating afforded by our chamber. These thick PEDOT-CI films are not observed to delaminate from any of the substrates investigated here. As revealed by four-point probe measurements, the sheet resistance of a 10 μm thick PEDOT-CI film on polyimide is 2 Ohms/square (conductivity 500 S/cm), meaning that this film has a low enough resistance to serve as an all-polymer, pseudocapacitive electrode without the need for a metal charge collector or a conductive carbon complement (Figure S2).<sup>21,22</sup>

Small selections of plant leaves and flower petals are identified as potential microstructured substrates on which to grow PEDOT-CI films. Lotus leaves display ordered arrays of

sharp pillars on their surface, which is responsible for their uniquely superhydrophobic surfaces. The surfaces of pansy and sunflower petals and leaves of the calathea zebrina plant contain pyramidal mesa structures. The leaves of pilea involucrata plants are densely textured with diverse surface features of varying sizes, in addition to an entangled mesh of fibers above the surface. Calathea zebrina and pilea involucrata are commonly available houseplants, and sunflowers are steadily stocked by florists. Dried, food-grade lotus leaves and pressed pansies are used in this study, due to availability.

Figure 2 shows scanning electron microscope (SEM) images of plant matter before and after vapor-coating with PEDOT-CI and optical images of plant matter partially coated with PEDOT-CI (the dark blue areas are PEDOT-CI coated and the other areas were masked with Teflon tape to prevent coating). SEM images of a PEDOT-CI film deposited on

polyimide are also shown for comparison. It is important to note that none of the substrates is carbonized, chemically altered, or otherwise damaged after being subjected to reactive vapor deposition. The optical images of partly coated plant matter in Figure 2 reveal that the uncoated parts of each leaf and flower petal look undamaged after being exposed to typical coating conditions. The substrates taken from live plants, sunflower petal, calathea zebrina leaf, and pilea involucreta leaf, lose less than 5% of their starting water content after being subjected to the standard vapor deposition conditions (heat and vacuum for approximately 40 min) used in this study. Stress–strain curves for a sunflower petal and pilea involucreta leaf before and after PEDOT-Cl coating (Figure S3) confirm that the process of reactive vapor deposition and the resulting PEDOT-Cl coating do not render these substrates brittle.

SEM images reveal that continuous, uniform coatings are conformally created on each substrate. Further, the structure of the underlying surface features for each leaf or flower petal is preserved after vapor-coating. Figure S4 shows a high-magnification SEM image to highlight the uniform and conformal coating on a single, sharp feature on a lotus leaf surface. SEM images of various features from the comparatively complicated surface of a pilea involucreta leaf are provided in Figure S5, in each case, the PEDOT-Cl coating tightly conforms to the topography and crevices of the surface features without filling any interstitial spaces.

These vapor-coated leaves and flower petals can serve as high-surface-area electrochemical electrodes for pseudocapacitive charge-storage devices. The PEDOT-Cl coating is the only electroactive component in this system and its associated redox reactions, electrochemical oxidation (doping) of residual PEDOT to the mixed polaron and bipolaron states of PEDOT-Cl (Figure 1) and electrochemical reduction (dedoping) of the bipolaron and/or polaron states of PEDOT-Cl to neutral PEDOT, serve as the chemical mechanisms by which charge can be stored in these films.

The pseudocapacitive performance of PEDOT-Cl electrodes is first quantified by performing two-electrode cyclic voltammetry (CV) in a liquid electrolyte (0.5 M aqueous H<sub>2</sub>SO<sub>4</sub>). On polyimide, nearly rectangular CV curves up to 500 mV/s and nearly triangular charge–discharge curves are recorded (Figure S6). No noticeable voltage drop is observed in the charge–discharge curve at a current density of 0.29 A/cm<sup>2</sup>, further confirming the low internal resistance of the 10 μm thick vapor-deposited PEDOT-Cl electrode material. Additionally, 68% of the initial capacitance (31 vs 21 F/cm<sup>2</sup>) is retained as the current density is increased from 0.29 to 2.32 A/cm<sup>2</sup>. Volumetric capacitances and energy and power densities calculated from these cyclic voltammograms by taking into account the total volume of two PEDOT-Cl electrodes are summarized in Table S1. Volumetric capacitances calculated from galvanostatic charge–discharge results are summarized in Table S2.

Cyclic voltammograms (Figure 3) and galvanostatic charge–discharge curves (Figure S7) of symmetric-electrode pseudocapacitors consisting of 10 μm thick PEDOT-Cl electrodes on plant matter reveal their increased energy-storage capacity as compared to polyimide substrates. An approximately linear correlation between the areal capacitance and the total surface area of the leaf and petal substrates is observed. A higher density of large-sized surface features leads to increased polymer mass loading and therefore higher areal capacitances (Table 1). The highest areal capacitances are obtained for

**Table 1. Areal Capacitance and Energy and Power Densities Derived from Cyclic Voltammograms (20 mV/s Scan Rate) of Two-Electrode Pseudocapacitors in 0.5 M H<sub>2</sub>SO<sub>4</sub> Electrolyte Using Various PEDOT-Cl-Coated (10 μm) Substrates as the Working and Counter Electrodes**

substrate	C (mF/cm <sup>2</sup> )	E (μW h/cm <sup>2</sup> )	P (mW/cm <sup>2</sup> )
polyimide	50	10.0	0.6
calathea zebrina leaf	86	17.2	1.1
lotus leaf	98	19.6	1.2
sunflower petal	110	22.0	1.3
pansy petal	128	25.6	1.5
pilea involucreta leaf	142	28.4	1.7

PEDOT-Cl-coated pilea involucreta leaves: an areal capacitance of 142 mF/cm<sup>2</sup> is measured, which is 3 times that of PEDOT-Cl electrodes on polyimide (50 mF/cm<sup>2</sup>). Accordingly, the areal energy density and power density exhibited by pilea leaf-based pseudocapacitors are increased by a factor of 3 compared to polyimide devices (Table 1). The areal capacitances of the PEDOT-Cl-coated leaves and petals reported herein are higher than those of state-of-the-art electrode materials, such as laser-scribed graphene (C<sub>areal</sub> 4–5 mF/cm<sup>2</sup>)<sup>12</sup> and hydrated graphite oxide (C<sub>areal</sub> 0.25 mF/cm<sup>2</sup>)<sup>28</sup> and are similar to that of carbide derived carbon films<sup>17</sup> (C<sub>areal</sub> 240 mF/cm<sup>2</sup> obtained from three-electrode CV measurements).

Moreover, above 94% of the initially observed capacitance of the vapor-deposited PEDOT-Cl film is maintained after 10 000 charge–discharge cycles on both polyimide and pilea involucreta substrates (Figure 3e). The recorded capacitances for PEDOT-Cl-coated pilea involucreta leaves are sometimes observed to increase upon continued charge–discharge cycling. This likely occurs because repeated charging–discharging actions rupture a few leaf cells, causing release of electrochemically active intracellular media and small molecules<sup>29</sup> into the conducting polymer film, which effectively increases the mass loading of redox-active materials and therefore electrode pseudocapacitance. Bending stability tests display the same phenomenon: the surface sheet resistances of PEDOT-Cl-coated pilea involucreta leaves are sometimes observed to decrease upon repeated bending (Figure 3f). Here, the mechanical force experienced during bending likely ruptures leaf cells and releases ion-conductive intracellular media into the conducting polymer film, leading to overall decreased resistances. Alternatively, mechanically induced annealing of the PEDOT-Cl coating could also be operative.

Three solid-state charge-storage devices are fabricated using PEDOT-Cl electrodes deposited on polyimide, pressed pansy petal, and pilea involucreta leaf substrates (Figure 4). A poly(vinyl alcohol)–sulfuric acid (PVA–H<sub>2</sub>SO<sub>4</sub>) gel is used as the solid-state electrolyte. For polyimide- and pansy petal-based devices, this gel electrolyte also serves as an effective electrode separator. For the comparatively rough pilea involucreta leaves, a porous Celgard 3500 membrane soaked with PVA–H<sub>2</sub>SO<sub>4</sub> gel is used as an electrode separator. The completed pansy petal and pilea involucreta leaf devices are packaged by laminating between two 10 μm thick poly(ethylene) films. An optical image of a laminated pilea involucreta leaf-based pseudocapacitor is shown in Figure 4e. The current–voltage responses and galvanostatic charge–discharge curves of the solid-state devices match those obtained in liquid electrolytes. The charge–discharge cycle

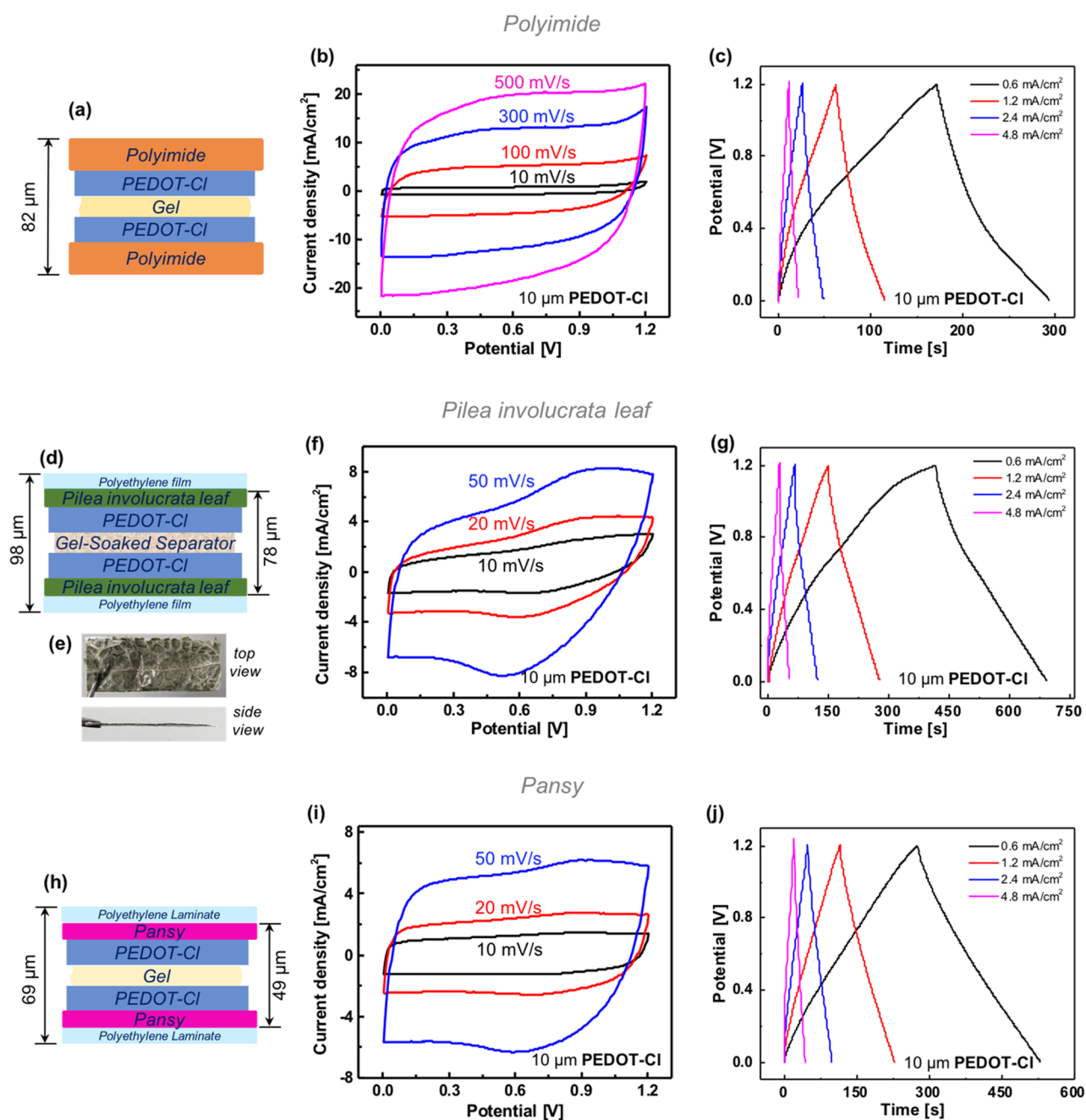


**Figure 4.** Solid-state electrochemical charge-storage devices. (a–j) For each panel: (left) cross-section of solid-state charge-storage device, (center) current–voltage response of the solid-state device, (right) galvanostatic charge–discharge curves for the solid-state device. PVA–H<sub>2</sub>SO<sub>4</sub> gel was used as the electrolyte in all solid-state devices. (e) Optical images of a packaged solid-state pseudocapacitor constructed with PEDOT-CI-coated pilea involucrata leaves.

stability of the pilea involucrata device is shown in Figure S8. Similar to liquid electrolyte devices, the capacitance is observed to occasionally increase with extended cycling and less than 5% loss in overall capacitance is observed after 10 000 charge–discharge cycles.

The performance of these solid-state charge-storage devices is contextualized using Ragone plots normalized to the area (Figure S9a) or volume (Figure S9b) of the entire device. The solid-state PEDOT-CI pseudocapacitors presented here rank among the highest known energy and power density devices containing aqueous or solid-state electrolytes.<sup>5–13,17,28,30–34</sup> A volumetric energy density of 4.7 mW h/cm<sup>3</sup> is achieved in pansy petal-based pseudocapacitors (power density 0.14 W/

cm<sup>3</sup>) (Tables S3 and S4). A volumetric power density of 3.2 W/cm<sup>3</sup> is obtained with polyimide substrates (energy density 0.36 mW h/cm<sup>3</sup>) (Tables S5 and S6). An areal energy density of 29 μW h/cm<sup>2</sup> (power density 0.9 mW/cm<sup>2</sup>) and areal power density of 26 mW/cm<sup>2</sup> (energy density 3.0 μW h/cm<sup>2</sup>) are obtained on pilea involucrata leaf and polyimide substrates, respectively (Tables S7 and S8).

## CONCLUSIONS

The naturally occurring surface features of selected plant leaves and flower petals can be exploited to create high-surface-area, microstructured all-polymer electrodes. The surfaces of plant matter can be nondestructively coated using reactive vapor

deposition, creating leaf- and petal-based all-polymer electrochemical electrodes in one step. Pseudocapacitive devices comprised of polymer-coated plant matter boast larger areal mass loadings of the electroactive material (Table S9) and proportionately higher areal capacitance compared to flat, planar substrates. Further, these plant-based pseudocapacitors display remarkable cycle stabilities, affirming that practical, lightweight (Table S10) charge-storage devices can be sustainably created using plant matter substrates and vapor-printed electroactive polymers.

## MATERIALS AND METHODS

**General Considerations.** All chemicals were purchased from Sigma-Aldrich or TCI America and used without further purification. Field-emission scanning electron microscopy was performed using a Magellan 400. Film thicknesses were measured on a Veeco Dektak 150 profilometer. Sheet resistance and conductivity were measured using a home-built four-point probe station. *Calathea zebrina* leaves, sunflower petals, and *Pilea involucrata* leaves were freshly cut from living plants, rinsed with water, and air-dried before use. Dry lotus leaves and pressed pansy petals were purchased and used without cleaning. Polyimide substrates were rinsed with isopropanol and air-dried before use.

**Film Preparation.** Films of p-doped poly(3,4-ethylenedioxythiophene) (PEDOT-CI) were directly deposited on 25  $\mu\text{m}$  thick polyimide substrates or plant matter using a previously described reaction chamber and process parameters<sup>8</sup> (Figure 1).<sup>26,27</sup> Typically, the oxidant flux was 1.5 times higher than the monomer flux. A significantly lower monomer rate resulted in a nonuniform film over a 5  $\times$  5 in.<sup>2</sup> substrate, whereas a significantly higher monomer rate sacrificed the conductivity of the resulting PEDOT-CI film. Argon gas was used to maintain the total pressure in the chamber of 300  $\pm$  10 mTorr, and the substrate stage temperature was strictly maintained at 150  $^{\circ}\text{C}$  during deposition. Nominally fragile plant matters were found to survive these chamber conditions with minimal damage and undetectable loss of natural water content (substrate stage temperatures of 170–180  $^{\circ}\text{C}$  were found to decrease the water content of plant matter and make them brittle). After the oxidant crucible was depleted of material, the vacuum was maintained until the substrate stage was cooled below 60  $^{\circ}\text{C}$ . The resulting PEDOT-CI films were immersed in 1 M  $\text{H}_2\text{SO}_4$  for 15 min to completely remove trapped iron salts and other reaction byproducts, as previously established (Figure S1).<sup>26,27</sup> Films obtained using this method remained p-doped even after rinsing/drying. Because of the iron(III) chloride oxidant used, chloride counterions were present in the as-deposited films.

Morphologically uniform 10  $\mu\text{m}$  thick films could be created on a variety of substrates over a total lateral area of up to 10 cm  $\times$  10 cm (limited by the size of the substrate stage). The maximum film thickness reported here, 10  $\mu\text{m}$ , is not determined by an innate material or process characteristic but rather by the practical fill capacity of the electrical furnace used in our chamber to vaporize  $\text{FeCl}_3$ . Use of a larger furnace with higher fill capacity should allow access to thicker films.

**Electrochemical Analysis of Symmetric PEDOT-CI Pseudocapacitors.** Symmetric PEDOT-CI pseudocapacitors with 0.5 M aqueous  $\text{H}_2\text{SO}_4$  or polymer gel electrolyte were characterized by two-electrode cyclic voltammetry and galvanostatic charge–discharge measurements using a WaveNow potentiostat and by electrochemical impedance spectroscopic analysis performed at open-circuit potential with a 10 mV amplitude.

**Calculations.** The volumetric or areal capacitances of symmetric devices were calculated from two-electrode cyclic voltammetry measurements using eq 1 or from galvanostatic charge–discharge curves using eq 2.

$$C_{\text{device}} = \frac{\int j \, d\nu}{\nu \Delta V} \quad (\text{F/cm}^3) \text{ or } (\text{F/cm}^2) \quad (1)$$

where  $V$  is the voltage,  $\nu$  is the scan rate,  $\Delta V$  is the voltage window, and  $j$  is the current density normalized to the total volume of two PEDOT electrodes (Table S1), to the total area of two PEDOT electrodes (Table 1), to the volume of the stacked device (Tables S3, S5, and S7), or to the area of the stacked device (Tables S4, S6, and S8).

$$C_{\text{device}} = \frac{I \Delta T}{\Delta V} \quad (\text{F/cm}^3) \quad (2)$$

where  $\Delta t$  is the discharge time,  $\Delta V$  is the voltage window, and  $I$  is the applied current density normalized to the total volume of two PEDOT electrodes (Table S2).

The energy density and power density were calculated using eqs 3 and 4, respectively.

$$E = \frac{0.5 C_{\text{device}} \Delta V^2}{3600} \quad (\text{W h/cm}^3) \text{ or } (\text{W h/cm}^2) \quad (3)$$

where  $\Delta V$  is the voltage window and  $C_{\text{device}}$  is the volumetric or areal capacitance of symmetric devices calculated from two-electrode cyclic voltammetry measurements using eq 1.

$$P = \frac{3600 E \nu}{\Delta V} \quad (\text{W/cm}^3) \text{ or } (\text{W h/cm}^2) \quad (4)$$

where  $E$  is the energy density normalized to the volume or area of a symmetric device,  $\nu$  is CV scan rate,  $\Delta V$  is voltage window.

**Fabrication of Solid-State PEDOT-CI Pseudocapacitors.** The gelled electrolyte was prepared by pouring 1 g of poly(vinyl alcohol) (PVA) (89 000–98 000, 99%, Sigma-Aldrich) into 10 g of 1 M  $\text{H}_2\text{SO}_4$  solution. The mixture was heated at 90  $^{\circ}\text{C}$  under vigorous stirring for 2 h. Solid-state device electrodes were prepared by pouring the polymer gelled electrolyte (100  $\mu\text{L/cm}^2$ ) onto PEDOT-CI-coated substrates and drying in air for 2 h. Two electrodes were then assembled face-to-face and left in air overnight until the electrolyte solidified. For the *Pilea involucrata* leaf-based pseudocapacitor, the same volume of the PVA– $\text{H}_2\text{SO}_4$  mixture was cast on a Celgard 3500 separator instead of being poured directly onto the coated leaf. The gel-soaked membrane was then sandwiched between two PEDOT-CI-coated *Pilea involucrata* leaves to create the final device. This extra step was necessary to avoid physical contact between the two fuzzy electrodes.

## ASSOCIATED CONTENT

### Supporting Information

The Supporting Information is available free of charge on the ACS Publications website at DOI: 10.1021/acsami.8b12551.

Tables of device capacitance and energy and power densities; scanning electron microscope images of vapor-coated plant matter (PDF)

## AUTHOR INFORMATION

### Corresponding Author

\*E-mail: tandrew@umass.edu.

### ORCID

Trisha L. Andrew: 0000-0002-8193-2912

### Author Contributions

The manuscript was written through contributions of all authors. All authors have given approval to the final version of the manuscript.

### Funding

This work was partially funded by the Air Force Office of Scientific Research under contract FA9550-14-1-0128. T.L.A. also gratefully acknowledges partial support by the David and Lucille Packard Foundation.

### Notes

The authors declare no competing financial interest.

## REFERENCES

- (1) Miller, J. R.; Simon, P. Electrochemical Capacitors for Energy Management. *Science* **2008**, *321*, 651–652.
- (2) Simon, P.; Gogotsi, Y.; Dunn, B. Where Do Batteries End and Supercapacitors Begin? *Science* **2014**, *343*, 1210–1211.
- (3) Armstrong, R. C.; Wolfam, C.; de Jong, K. P.; Gross, R.; Lewis, N. S.; Boardman, B.; Ragauskas, A. J.; Ehrhardt-Martinez, K.; Crabtree, G.; Ramana, M. V. The Frontiers of Energy. *Nat. Energy* **2016**, *1*, No. 15020.
- (4) Elliott, D. A Balancing Act for Renewables. *Nat. Energy* **2016**, *1*, No. 15003.
- (5) Zhu, Y.; Murali, S.; Stoller, M. D.; Ganesh, K. J.; Cai, W.; Ferreira, P. J.; Pirkle, A.; Wallace, R. M.; Cychosz, K. A.; Thommes, M.; Su, D.; Stach, E. A.; Ruoff, R. S. Carbon-Based Supercapacitors Produced by Activation of Graphene. *Science* **2011**, *332*, 1537–1541.
- (6) Chmiola, J.; Yushin, G.; Gogotsi, Y.; Portet, C.; Simon, P.; Taberna, P. L. Anomalous Increase in Carbon Capacitance at Pore Sizes Less Than 1 Nanometer. *Science* **2006**, *313*, 1760–1763.
- (7) Acerce, M.; Voiry, D.; Chhowalla, M. Metallic 1T Phase MoS<sub>2</sub> Nanosheets as Supercapacitor Electrode Materials. *Nat. Nanotechnol.* **2015**, *10*, 313–318.
- (8) Lukatskaya, M. R.; Mashtalir, O.; Ren, C. E.; Dall'Agnese, Y.; Rozier, P.; Taberna, P. L.; Naguib, M.; Simon, P.; Barsoum, M. W.; Gogotsi, Y. Cation Intercalation and High Volumetric Capacitance of Two-Dimensional Titanium Carbide. *Science* **2013**, *341*, 1502–1505.
- (9) Ghidui, M.; Lukatskaya, M. R.; Zhao, M.-Q.; Gogotsi, Y.; Barsoum, M. W. Conductive Two-dimensional Titanium Carbide 'Clay' with High Volumetric Capacitance. *Nature* **2014**, *516*, 78–81.
- (10) Yang, X.; Cheng, C.; Wang, Y.; Qiu, L.; Li, D. Liquid-Mediated Dense Integration of Graphene Materials for Compact Capacitive Energy Storage. *Science* **2013**, *341*, 534–537.
- (11) Augustyn, V.; Come, J.; Lowe, M. A.; Kim, J. W.; Taberna, P.-L.; Tolbert, S. H.; Abruña, H. D.; Simon, P.; Dunn, B. High-rate Electrochemical Energy Storage Through Li<sup>+</sup> Intercalation Pseudocapacitance. *Nat. Mater.* **2013**, *12*, 518–522.
- (12) El-Kady, M. F.; Strong, V.; Dubin, S.; Kaner, R. B. Laser Scribing of High-Performance and Flexible Graphene-Based Electrochemical Capacitors. *Science* **2012**, *335*, 1326–1330.
- (13) El-Kady, M. F.; Ihms, M.; Li, M.; Hwang, J. Y.; Mousavi, M. F.; Chaney, L.; Lech, A. T.; Kaner, R. B. Engineering Three-dimensional Hybrid Supercapacitors and Microsupercapacitors for High-performance Integrated Energy Storage. *Proc. Natl. Acad. Sci. U.S.A.* **2015**, *112*, 4233–4238.
- (14) Kim, J.; Lee, J.; You, J.; Park, M.-S.; Hossain, M. S. A.; Yamauchi, Y.; Kim, J. H. Conductive Polymers for Next-generation Energy Storage Systems: Recent Progress and New Functions. *Mater. Horiz.* **2016**, *3*, 517–535.
- (15) Mike, J. F.; Lutkenhaus, J. L. Recent Advances in Conjugated Polymer Energy Storage. *J. Polym. Sci., Part B: Polym. Phys.* **2013**, *51*, 468–480.
- (16) Indrajit, S.; Abhijit, G.; Li-Chyong, C.; Kuei-Hsien, C. Conducting Polymer-based Flexible Supercapacitor. *Energy Sci. Eng.* **2015**, *3*, 2–26.
- (17) Huang, P.; Lethien, C.; Pinaud, S.; Brousse, K.; Laloo, R.; Turq, V.; Respaud, M.; Demortière, A.; Daffos, B.; Taberna, P. L.; Chaudret, B.; Gogotsi, Y.; Simon, P. On-chip and Freestanding Elastic Carbon Films for Micro-Supercapacitors. *Science* **2016**, *351*, 691–695.
- (18) Yuan, L.; Yao, B.; Hu, B.; Huo, K.; Chen, W.; Zhou, J. Polypyrrole-coated Paper for Flexible Solid-state Energy Storage. *Energy Environ. Sci.* **2013**, *6*, 470–476.
- (19) Liu, A.; Kovacic, P.; Peard, N.; Tian, W.; Goktas, H.; Lau, J.; Dunn, B.; Gleason, K. K. Monolithic Flexible Supercapacitors Integrated into Single Sheets of Paper and Membrane via Vapor Printing. *Adv. Mater.* **2017**, *29*, No. 1606091.
- (20) Fong, K. D.; Wang, T.; Smoukov, S. K. Multidimensional Performance Optimization of Conducting Polymer-based Supercapacitor Electrodes. *Sustainable Energy Fuels* **2017**, *1*, 1857–1874.
- (21) Li, Z.; Ma, G.; Ge, R.; Qin, F.; Dong, X.; Meng, W.; Liu, T.; Tong, J.; Jiang, F.; Zhou, Y.; et al. Free-Standing Conducting Polymer Films for High-Performance Energy Devices. *Angew. Chem., Int. Ed.* **2016**, *55*, 979–982.
- (22) Xu, Y.; Tao, Y.; Zheng, X.; Ma, H.; Luo, J.; Kang, F.; Yang, Q.-H. A Metal-Free Supercapacitor Electrode Material with a Record High Volumetric Capacitance over 800 F cm<sup>-3</sup>. *Adv. Mater.* **2015**, *27*, 8082–8087.
- (23) Mike, J. F.; Lutkenhaus, J. L. Electrochemically Active Polymers for Electrochemical Energy Storage: Opportunities and Challenges. *ACS Macro. Lett.* **2013**, *2*, 839–844.
- (24) Wu, G.; Tan, P.; Wang, D.; Li, Z.; Peng, L.; Hu, Y.; Wang, C.; Zhu, W.; Chen, S.; Chen, W. High-Performance Supercapacitors Based on Electrochemical-Induced Vertical-Aligned Carbon Nanotubes and Polyaniline Nanocomposite Electrodes. *Sci. Rep.* **2017**, *7*, No. 43676.
- (25) Yan, X.; Tai, Z.; Chen, J.; Xue, Q. Fabrication of Carbon Nanofiber–Polyaniline Composite Flexible Paper for Supercapacitor. *Nanoscale* **2011**, *3*, 212–216.
- (26) Zhang, L.; Fairbanks, M.; Andrew, T. L. Rugged Textile Electrodes for Wearable Devices Obtained by Vapor Coating Off-the-Shelf, Plain-Woven Fabrics. *Adv. Funct. Mater.* **2017**, *27*, No. 1700415.
- (27) Zhang, L.; Andrew, T. L. Deposition Dependent Ion Transport in Doped Conjugated Polymer Films: Insights for Creating High-Performance Electrochemical Devices. *Adv. Mater. Interfaces* **2017**, *4*, No. 1700873.
- (28) Beidaghi, M.; Wang, C. Micro-Supercapacitors Based on Interdigital Electrodes of Reduced Graphene Oxide and Carbon Nanotube Composites with Ultrahigh Power Handling Performance. *Adv. Funct. Mater.* **2012**, *22*, 4501–4510.
- (29) Muñoz-Huerta, R. F.; Ortiz-Melendez, A. J.; Guevara-Gonzalez, R. G.; Torres-Pacheco, I.; Herrera-Ruiz, G.; Contreras-Medina, L. M.; Prado-Olivarez, J.; Ocampo-Velazquez, R. V. An Analysis of Electrical Impedance Measurements Applied for Plant N Status Estimation in Lettuce (*Lactuca sativa*). *Sensors* **2014**, *14*, No. 11492.
- (30) Wu, Z.-S.; Parvez, K.; Feng, X.; Müllen, K. Graphene-based In-plane Micro-supercapacitors with High Power and Energy Densities. *Nat. Commun.* **2013**, *4*, No. 2487.
- (31) Pech, D.; Brunet, M.; Durou, H.; Huang, P.; Mochalin, V.; Gogotsi, Y.; Taberna, P.-L.; Simon, P. Ultrahigh-power Micrometre-sized Supercapacitors Based on Onion-like Carbon. *Nat. Nanotechnol.* **2010**, *5*, 651–654.
- (32) El-Kady, M. F.; Kaner, R. B. Scalable Fabrication of High-power Graphene Micro-supercapacitors for Flexible and On-chip Energy Storage. *Nat. Commun.* **2013**, *4*, No. 1475.
- (33) Meng, C.; Maeng, J.; John, S. W. M.; Irazoqui, P. P. Ultrasmall Integrated 3D Micro-Supercapacitors Solve Energy Storage for Miniature Devices. *Adv. Energy Mater.* **2014**, *4*, No. 1301269.
- (34) Qu, G.; Cheng, J.; Li, X.; Yuan, D.; Chen, P.; Chen, X.; Wang, B.; Peng, H. A Fiber Supercapacitor with High Energy Density Based on Hollow Graphene/Conducting Polymer Fiber Electrode. *Adv. Mater.* **2016**, *28*, 3646–3652.